Anat Sci Int (2017) 92:267–274
DOI 10.1007/s12565-016-0332-3

ORIGINAL ARTICLE

Stereological assessment of normal Persian squirrels (*Sciurus anomalus*) kidney

Mohsen Akbari[1] · Nader Goodarzi[1] · Majid Tavafi[2]

Received: 8 November 2015 / Accepted: 3 February 2016 / Published online: 19 February 2016

Abstract The functions of the mammalian kidney are closely related to its structure. This suggests that renal function can be completely characterized by accurate knowledge of its quantitative morphological features. The aim of this study was to investigate the histomorphometric features of the kidney using design-based and unbiased stereological methods in the Persian squirrel (*Sciurus anomalus*), which is the only representative of the Sciuridae family in the Middle East. The left kidneys of five animals were examined. Total volume of the kidney, cortex, and medulla were determined to be 960.75 ± 87.4, 754.31 ± 77.09 and 206.1 ± 16.89 mm^3, respectively. The glomerular number was 32844.03 ± 1069.19, and the total glomerular volume was estimated to be 36.7 ± 1.45 mm^3. The volume and length of the proximal convoluted tubule were estimated at 585.67 ± 60.7 mm^3 and 328.8 ± 14.8 m, respectively, with both values being greater than those reported in the rat kidney. The volume and length of the distal convoluted tubule were calculated at 122.34 ± 7.38 mm^3 and 234.4 ± 17.45 m, respectively, which are also greater than those reported in the rat kidney. Despite the comparable body weight, the total number and mean individual volume of glomeruli in the Persian squirrel kidney were greater than those in the rat kidney. Overall, the stereological variables of the kidneys elucidated in this study are exclusive to the Persian squirrel. Our findings, together with future renal physiological data, will contribute to a better understanding of the renal structure–function relationship in the Persian squirrel.

Keywords Persian squirrel · Kidney · Morphometry · Stereology · Quantitative study

✉ Nader Goodarzi
n.goodarzi@razi.ac.ir

[1] Department of Basic Science, Faculty of Veterinary Medicine, Razi University, Kermanshah, Iran

[2] Department of Anatomy, Faculty of Medicine, Lorestan University of Medical Sciences, Khoram Abad, Iran

Introduction

Mammalian kidneys play a dominant role in controlling both the volume and concentration of body fluids (Alkahtani et al. 2004). Mammalian species in arid and semi-arid habitats, where the availability of free water not only tends to be limited or scarce but also to vary temporally, are continually faced with the problem of water conservation (El-Gohary et al. 2011).

A great deal of effort has been expended in the measurement of the transport properties of renal tubular membranes (Kokko 1974; Jamison 1976). Such investigations have resulted in considerable advances in the understanding of the mechanism of urine formation by the kidney. This function, however, cannot be completely characterized without knowledge of the number and dimensions of the renal tubules at various levels of the kidney as well as the volume of the interstitial and vascular spaces. Precise estimates of these parameters have recently been reported for the kidneys of many different species, and numerous structural differences among species are becoming evident. For example, three types of renal corpuscles have been described in the dog (Beeuwkes 1971), human (Beeuwkes 1980), rabbit (Kaissling and Kriz 1979), and the sand rat *Psammomys obesus* (Bankir et al. 1979) based on their position in the renal cortex and the pattern of their efferent vessels. Other studies have reported on the morphological and morphometrical features of the kidneys in various rodent species, including the rat (Bertram et al. 1992), rabbit (Knepper et al. 1977), and guinea pig (Al-Sharoot 2014).

The Persian squirrel (*Sciurus anomalus*), the only representative of the Sciuridae family in the Middle East, is a herbivorous animal feeding mostly on pine acorns and other seeds and fruits. It is a wild species but has in recent times become a common household pet, and referrals to veterinary hospitals have increased (Khazraiinia et al. 2008). To our knowledge, only one study has been published on the radiographic anatomy of the urinary system of this species (Veshkini et al. 2011), and no data are currently available on the histomorphometric features of its kidneys. The aim of our study was to quantify the histomorphometric properties of the kidneys in the Persian squirrel using design-based and unbiased stereological procedures. These findings should lead to a deeper understanding of the structure–function relationships of the urinary system in this species.

Materials and methods

Animals and tissue preparation

Five male Persian squirrel were used in our study, and approval for the investigation was obtained by the ethics committee of Faculty of Veterinary Medicine Razi University (No.: 94/577/1;208). The animals were euthanized and their left kidneys removed. Perirenal fat and connective tissue were first removed from the kidneys, and the kidneys were then weighed and the primary volume measured using the immersion method (Silva and Merzel 2001), following which the kidneys were fixed in 10 % neutral buffered formaldehyde for 5 days. The reference volume or final volume of the kidney should be estimated in a stereological study to prevent the reference trap (Braendgaard and Gundersen 1986; Gundersen et al. 1988a). The Cavalieri technique, which is the most relevant method of reference volume estimation, needs consecutive sections, but it is time-consuming method. Thus, the reference volume was estimated by calculating shrinkage after tissue processing and staining without the need for serial sections. Estimation of the shrinkage and tubule length requires isotropic uniform random sections (Gundersen et al. 1988a; Nyengaard 1999). These sections were achieved by the orientator method (Fig. 1). Briefly, each kidney was placed on a circle of which each half was divided into ten equal distances (φ-clock); a random number between zero and ten was selected and the kidney sectioned into two halves usinga blade in that direction (Fig. 1a). The cut surface of the one half of the kidney was then placed on the 0–0 direction of the second circle with ten unequal sinus-weighted divisions (θ-clock) and the second cut done by selecting a random number (Fig. 1b). The cut surface of the other half of the kidney was placed vertically on the θ-clock. The second cut was done by selecting a random number (Fig. 1c). The entire kidney was sectioned into slabs with a blade, placed in the direction of the second cuts at an spacing of 1 mm. Then the slabs (7–10 slabs) were collected. A circle was punched into a kidney slab using a trocar (Fig. 2). The diameter of each circular piece of the kidney was measured by a micrometer, and the area of the circle was estimated using

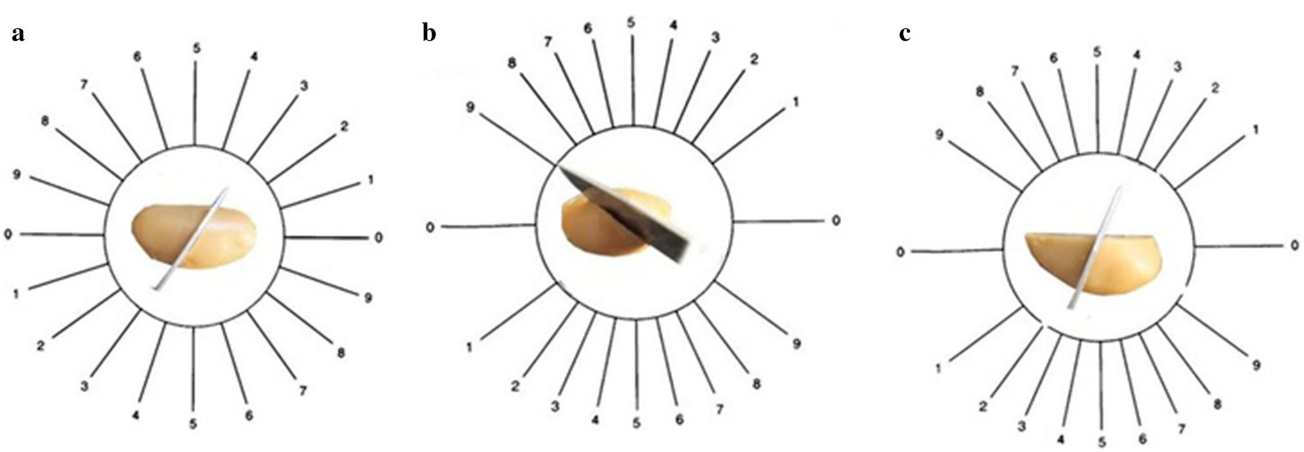

Fig. 1 Orientator method for generating isotropic uniform random sections. **a** Each kidney was placed on a circle of which each was divided into 10 equal distances (φ-clock). A random number between 0 and 10 was selected, and the kidney was sectioned into two halves using a blade in that direction (here *3*). **b** The cut surface of the one half of the kidney was placed vertically on the θ-clock with 10 unequal sinus-weighted divisions. The second cut done by selecting a random number (here *9*). **c** The cut surface of the other half of the kidney was then placed parallel to the 0–0 direction of the θ-clock and the second cut done by selecting a random number (here *3*). The entire kidney was sectioned into slabs with a blade placed in the direction of the second cuts

Fig. 2 Between 7 and 10 slabs were obtained from the kidney. A trocar was used to punch a circle from a kidney slab. The diameters of the circular piece of the kidney and the area of the circle were then estimated

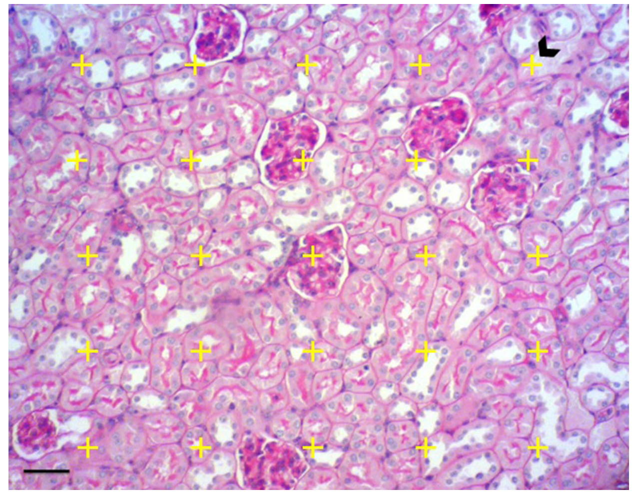

Fig. 3 A microscopic section of kidney showing the glomerulus, proximal convoluted tubules (PCT), distal convoluted tubules (DCT), connective tissue, and vessels. To estimate the volume density of these parameters, we divided the total number of points hitting each component (the point is the *right upper corner* of the *cross*, i.e., the *thick black arrow*) by the total number of points hitting the reference space. *Scale bar* 100 μm

the standard formula for calculating the area of a circle. The slabs and circular piece were embedded in paraffin, and sections (thickness 5 μm) were prepared and stained (Periodic Acid–Schiff). After staining, the area of the circular piece was measured again and volume shrinkage was calculated from Eq. (1) (Nyengaard 1999):

$$\text{Volume shrinkage} := 1 - \left(\frac{\mathrm{AA}}{\mathrm{AB}}\right)^{1.5} \quad (1)$$

where AA and AB are the area of the circular piece after and before processing, sectioning, and staining respectively. After estimating the shrinkage, we corrected the final volume of the kidney (the reference space) using Eq. (2).

$$V_{\mathrm{final}} := V_{\mathrm{primary}} \times (1 - \text{volume shrinkage}) \quad (2)$$

Stereological study

Estimation of fractional and total volume (absolute volume)

All sections obtained as described in the previous section were analyzed using a videomicroscopy system equipped with a microscope (model CX2; Olympus, Tokyo, Japan) connected to a video camera (Dino-Lite—Dinocapture ver. 5; 30.5 mm; AnMo Electronics Corp., New Taipei City, Taiwan), a Dell Pentium 4 PC (Dell Inc., Round Rock, TX) and a flat monitor to determine the parameters. The point probe (10 × 10-cm frame with 20 points) was superimposed upon the images of the tissue sections viewed on the monitor, and a volume density (V_v) of the renal cortex, medulla, glomeruli, proximal convoluted tubule, distal convoluted tubule, collecting ducts, Henle's loop, vessels, and connective tissue were obtained using a point-counting method and (Fig. 3) and Eq. (3) (Gundersen et al. 1988a) as follows:

$$V_v := \frac{P_{\mathrm{structure}}}{P_{\mathrm{reference}}} \quad (3)$$

where '$P_{\mathrm{structure}}$' and '$P_{\mathrm{reference}}$' were the number of test points falling on the structure's profile and on the reference space, respectively. Between 10 and 14 microscopic fields were examined in each kidney. The absolute volume of the parameters was estimated by multiplying the fractional volume by the final volume of the kidney to prevent the reference trap (Nyengaard 1999; Mandarim-de-Lacerda 2003).

Estimation of length density and total length of renal tubules

The length density of the proximal and distal convoluted tubules, collecting ducts, Henle's loop, and vessels was estimated by randomly overlaying an unbiased counting frame with exclusion lines (the left and lower borders) and

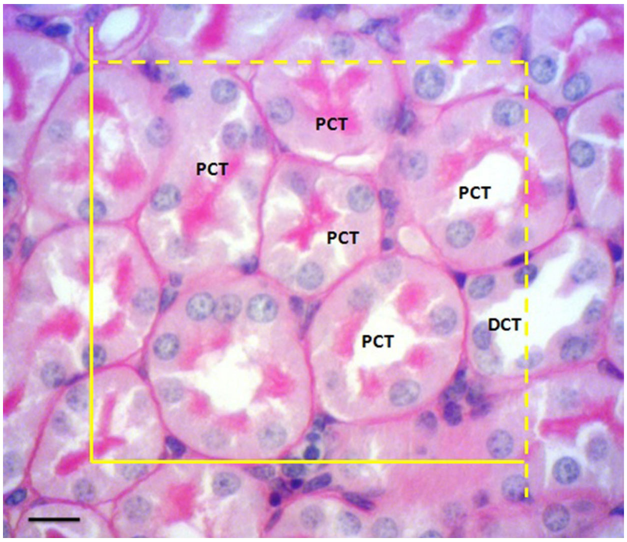

Fig. 4 The length density of the renal tubules is estimated by superimposing an unbiased counting frame with inclusion (*dashed lines*) and exclusion (*unbroken lines*) on the images of the tissue sections. The tubule profiles completely inside the counting frame or partly inside the counting frame but only touching the inclusion lines are counted (here 5 PCT and 1 DCT). The tubule profiles touching the exclusion lines and its extensions are ignored. *Scale bar* 100 μm

inclusion lines (the right and upper borders) (Nyengaard 1999; Mandarim-de-Lacerda 2003) with an area of 100 cm^2 on the monitor live images. The tubule and vessel profiles completely or partly inside the counting frame but only touching the inclusion lines were counted (Fig. 4). The length density of each profile was calculated from Eq. (4):

$$L_v := 2 \times \frac{\sum Q}{a(\text{frame}) \times \sum \text{frame}} \tag{4}$$

where $\sum Q$ is the total number of the tubule profiles counted per kidney, a(frame) equals the area associated with a frame, and $\sum$frame is the total number of frames counted. Finally, the total length of each tubule in the kidney, L, was calculated by multiplying the length density (L_v) by the total volume of the kidney.

Estimation of numerical density and total glomerular number

The total number of glomeruli per kidney was estimated using the physical disector method (Sterio 1984). From each kidney, a section pair 30 μm apart (the first and seventh sections) was obtained. Two separate projecting systems with similar equipment were used. Two disector probes (740 × 740 μm) with exclusion lines (the left and lower borders) and inclusion lines (the right and upper borders) were superimposed on the images of the first section as the reference section (Fig. 5a) and the seventh section as the look-up section (Fig. 5b) at a total magnification of 135×. A glomerulus was counted if it was present in reference section but not in the look-up section and did not touch the exclusion lines. At least 100 glomeruli per kidney were counted. The numerical density of the glomeruli was estimated using Eq. (5).

$$N_V := \frac{\sum Q^-}{a(\text{frame}) \times h \times \sum P} \tag{5}$$

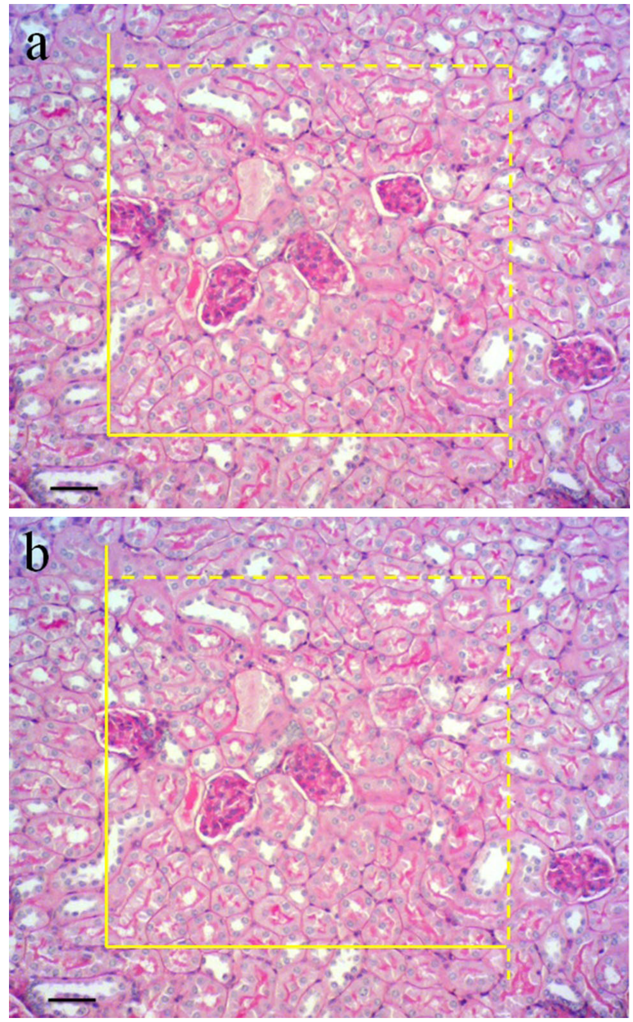

Fig. 5 For estimating the numerical density of glomeruli according to the physical disector method, the images of two sections 30 μm apart (first and seventh sections) were used as the reference section (**a**) and look-up section (**b**), respectively. An unbiased counting frame is superimposed on the sample sections. Glomerular profiles are counted if they are contained completely or partly in the frame and do not touch the exclusion (*unbroken lines*) as well as if they are disappeared in the look-up section (only 1 such glomerular profile here). *Scale bar* 50 μm

where $\sum Q^{-}$ denotes the number of counted glomeruli, a (frame) is the area of the disector frame, $\sum P$ is the sum of studied field, and h is the disector height. Total glomerular number was estimated by multiplying the numerical density (N_v) by the reference volume (renal cortex).

In addition, we estimated the mean individual glomerular volume, using Eq. (6) (Gundersen et al. 1988b):

$$V_G := \frac{V_v}{N_v} \tag{6}$$

where V_v and N_v are the volume density and numerical density of glomeruli, respectively.

Statistical analysis

Statistical analysis was performed using SPSS software v.22 (IBM Corp., Armonk, NY) and the one-sample t test to compare our results obtained in the Persian squirrel and previous reports in the rat. Two-tailed P values of <0.05 were considered to be statistically significant. The coefficient of error (CE) was calculated for all variables from Eq. (7) (Howard and Reed 1998).

$$\mathrm{CE} = \frac{\mathrm{SD}}{\sqrt{n} \cdot \mathrm{mean}} \tag{7}$$

Results

The kidney of the Persian squirrel has the typical bean-shaped appearance which is a characteristic of unilobar mammalian kidneys. The absolute volume of the kidney, cortex, medulla, glomeruli, and interstitial connective tissue are presented in Table 1, and the absolute volume and length of the proximal and distal convoluted tubules, collecting ducts, loop of Henle, and vessels are presented in Table 2. The total number of glomeruli, volume, and mean individual glomerular volume are shown in Table 3. All measurements are presented as the mean ± standard deviation (SD). The mean kidney weight and the primary volume obtained through the Archimedean principles of liquid dynamics (Immersion method,) were 1.18 ± 0.19 g and 1.1 ± 0.18 mm^3, respectively. As a result, the renal density was found to be 1.07 ± 0.03. The present findings show that the total volume of the Persian squirrel kidney was 960.75 ± 172.88 mm^3, of which 754.3 97 mm^3 was occupied by the renal cortex and 260.1 ± 16.89 mm^3 was related to the renal medulla. The Persian squirrel kidney contained on average 64.3 ± 4.36 mm^3 of interstitial connective tissue and 40.68 ± 1.89 mm^3 of blood vessels. The total length of vessels was estimated to be 432.66 ± 39.72 m. The total number of glomeruli in the normal Persian squirrel kidney was found to be 32,844 ± 1069 with a glomerular volume of 36.72 ± 1.45 mm^3. The mean individual glomerular volume was estimated to be 11 × 10^{-4} ± 0.82 mm^3 The CE for all of the stereological variables fell within acceptable range of <5 %.

Discussion

It has been well established that water availability is limited or scarce in arid and semi-arid habitats. Thus, the different animal species which live in these environments are faced with the problem of water conservation. The means by which such animals achieve efficient water economy can be determined through examination of the ability of the kidney to produce a concentrated urine (Weissenberg and Shkolnik 1994).

The integration of morphological and functional observations continues to provide valuable new insight into the mechanisms by which the kidney performs its varied and intricate tasks. In this study, design-base and unbiased stereological methods were used to determine the absolute values of the histomorphometric features of the normal renal tissue in the Persian squirrel (*Sciurus anomalus*).

We calculated the renal density of the Persian squirrel to be 1.07 ± 0.03. These results are in agreement with those of Christiansen et al. (1997), who reported that 1 g of renal weight was equivalent to 1 ml of renal volume. Bolat et al. (2011) pointed out that formalin fixation causes rabbit kidney tissue to swell, with a subsequent increase in the weight and volume. In another study, Malas et al. (2002) reported the renal density of the male rat to be 1.19. The mean value of tissue shrinkage in our was calculated to be 0.17 ± 0.07.

Table 1 Weight and total volume of the kidney and its subcomponents in the Persian squirrel (*Sciurus anomalus*)

Total weight and volume of left kidney[a]		Volume of components of left kidney		
Weight (g)	Total volume (mm^3)	Cortical volume (mm^3)	Medulla volume (mm^3)	Interstitial volume (mm^3)
1.18 ± 0.19	960.75 ± 87.4 (4 %)	754.31 ± 77.09 (4.6 %)	206.1 ± 16.89 (3.7 %)	64.3 ± 4.36 (3 %)

Data are presented as the mean ± standard deviation (SD)

[a] Coefficient error (CE) is given in parenthesis

Table 2 Total volume and length of the proximal and distal convoluted tubules, collecting ducts, loop of Henle, and vessels in the kidney of the Persian squirrel

Parameters	Proximal convoluted tubule	Distal convoluted tubule	Collecting ducts	Loop of Henle	Vessels in the kidney
Volume (mm^3)	585.67 ± 60.7	122.34 ± 7.38	121.32.8 ± 11.52	32.18 ± 3.24	40.63 ± 1.89
CE (%)	4.5	2.6	4.2	4.5	0.2
Length (m)	328.8 ± 14.8	234.4 ± 17.45	341.35 ± 36.58	191.5 ± 18.26	732.66 ± 39.72
CE (%)	2	3.3	4.8	4.2	4.1

Data are presented as the mean ± SD, unless indicated otherwise

Table 3 The total number, total volume (mm^3) and mean individual volume (10^{-4} mm^3) of glomeruli in the Persian squirrel kidney are shown as mean ± standard deviation

Parameters of the glomeruli[a]		
Total number	Total volume	Mean individual volume
32844.03 ± 1069.19 (1.4 %)	36.7 ± 1.45 (1.7 %)	11 ± 0.82 (3.34 %)

Data are presented as the mean ± SD

[a] CE is given in parenthesis

The absolute volume of the kidney in the Persian squirrel determined in our study, namely, 960.75 ± 172.8 mm^3, is significantly ($P = 0.047$) greater than that reported for the rat kidney (678 ± 54 mm^3; Soleimani and Tavakolyan 2013). Accordingly, the total volume of the cortex and medulla were also significantly ($P = 0.015$ and $P = 0.001$) greater than those in the rat kidney (510 ± 41 and 167 ± 26 mm^3, respectively; Soleimani and Tavakolyan 2013). It is worth nothing that medullary thickness and cortico/-medullary ratio play an important role in the renal function and its urine-concentrating ability. In general, the kidneys of mammals in arid habitats tend to have a relatively thicker medulla and maximum urine concentration ability compared to those of mammals in mesic and freshwater habitats (Beuchat 1996). Our calculations therefore suggest that the kidney of the Persian squirrel has a higher urine-concentrating ability than that of the rat.

Although the cortical thickness and cortical area would be more sensitive and accurate parameters than renal bipolar length to predict the presence of renal disease (Tsushima et al. 2001), the thickness of the cortex or parenchyma of the kidney may provide biased data since the third dimension is omitted. Lodrup et al. (2008) showed that structural parameters, such as cortical volume and glomerular volume, are significantly and positively correlated with glomerular filtration rate (GFR). Therefore, volume estimation and three-dimensional imaging are necessary to evaluate normal or pathological conditions.

Number is one of the most important parameters which can be used to elucidate the relation between a structure and its function (Kaplan et al. 2012). It has been shown that a reduction in the number of nephrons, i.e., the volume of cortex, may cause high blood pressure and kidney failure (Brenner and Chertow 1993). In our study, the total number of glomeruli (32844 ± 1069) and the total glomerular volume (36.7 ± 1.45 mm^3) in the Persian squirrel kidney was significantly ($P = 0.003$ and $P = 0.001$) higher than those of the rat (27912.3 ± 1558 and 25.6 ± 1.029 mm^3, respectively; Tavafi et al. 2011). A strong positive correlation has been found between body weight and glomerular number, and a significant positive correlation has been found between body weight and kidney weight (Nyengaard and Bendtsen 1990). We found the mean body weight and kidney weight of the Persian squirrels measured in our study to be 255 ± 10.8 and 1.18 ± 0.19 g, respectively. These findings show that despite the comparable body weight of the Persian squirrel and rat, their kidney weight and kidney volume are significantly different ($P = 0.047$). Moreover, the glomeruli of the Persian squirrel in our study are significantly ($P = 0.002$) larger ($11 \pm 0.81 \times 10^{-4}$ mm^3) than those reported in the rat ($6.72 \pm 0.98 \times 10^{-4}$ mm^3; Heilmann et al. 2012). According to these results, the larger filtration surface area of the Persian squirrel may provide certain adaptive advantages as the GFR is basically dependent on the external surface area of glomeruli.

It is important to note the advantages of the physical disector procedure as a method for counting glomeruli. No assumptions of glomerular shape, size, uniformity of size, or orientation are required in this method. Furthermore, the estimates are not influenced by the shrinkage or swelling artifacts associated with tissue processing. This is an especially important consideration when, for example, damaged glomeruli are being examined since their shrinkage or swelling features may well be different from those of normal glomeruli. On the other hand, section thickness need not be determined and the estimates are not influenced by section compression (Bertram et al. 1992).

Based on the results obtained in our study, both the volume (585.67 ± 60.7 mm^3) and the total length (328 ± 14.8 m) of the proximal convoluted tubule in the Persian squirrel are significantly ($P = 0.003$ and $P = 0.002$) greater than those estimated in the rat kidney (312 ± 59 mm^3 and 247 ± 38 m, respectively; Rasch and Dorup 1997). An interesting finding was that both the volume (122.3 ± 7.38 mm^3) and length (234.4 ± 17.45 m) of the distal convoluted tubule are also significantly ($P = 0.001$ and $P = 0.001$) greater than those reported for the rat kidney (70 ± 29 mm^3 and 131 ± 22 m, respectively; Rasch and Dorup 1997). Due to the physiological role of these renal tubules in the reabsorption of Na^+, water, glucose, and proteins and the secretion of K^+ and H^+, the chemical characteristics of the urine and its constituents in the Persian squirrel could be specific and different from those of the rat.

All of the structural parameters reported here were obtained in a design-based manner, which is the golden standard in stereology. As such, they provide solid basic knowledge of the three-dimensional morphometry of renal tissue in the Persian squirrel. Further investigations at the electron microscope level associated with urine analysis are needed to complete our results and to achieve a better understanding of the structure–function relation of the urinary system in the Persian squirrel.

Acknowledgments This article was extracted in part from the thesis prepared by Mohsen Akbari to fulfill the requirements required for earning the DVM degree. The authors gratefully acknowledge the financial support for this work that was provided by Razi University. They are also grateful to Mr. Milad Azarhoosh for his valuable assistance in preparing the photographs.

Compliance with ethical standards

Conflict of interest None.

References

Alkahtani MA, Zoleta C, Caviedes-Vidal E, Garland T (2004) Kidney mass and relative medullary thickness of rodents in relation to habitat, body size, and phylogeny. Physiol Biochem Zool 77(3):346–365

Al-Sharoot HA (2014) Morphological and histological study of the kidney in guinea pig. Int J Rec Sci Res 5:1973–1976

Bankir L, Kaissling B, de Rouffignac C, Kriz W (1979) The vascular organization of the kidney of *Psammomys obesus*. Anat Embryol 155:149–190

Beeuwkes R (1971) Efferent vascular patterns and early vascular-tubular relations in the dog kidney. Am J Physiol 221:361–374

Beeuwkes R (1980) The vascular organization of the kidney. Annu Rev Physiol 42:521–542

Bertram JF, Soosaipillai MC, Ricardo SD, Ryan GB (1992) Total numbers of glomeruli and individual glomerular cell types in the normal rat kidney. Cell Tissue Res 270:37–45

Beuchat CA (1996) Structure and concentrating ability of the mammalian kidney: correlations with habitat. Am J Physiol 271:157–179

Bolat D, Bahar S, Selcuk ML, Tipirdamaz S (2011) Morphometric investigations of fresh and fixed rabbit kidney. Eurasian J Vet Sci 27:149–154

Braendgaard H, Gundersen HJ (1986) The impact of recent stereological advances on quantitative studies of the nervous system. J Neurosci Methods 18:39–78

Brenner BM, Chertow GM (1993) Congenital oligonephropathy: an inborn cause of adult hypertension and progressive renal injury? Curr Opin Nephrol Hypertens 2:691–695

Christiansen T, Rasch R, Stødkilde-Jørgensen H, Flyvbjerg A (1997) Relationship between MRI and morphometric kidney measurements in diabetic and non-diabetic rats. Kidney Int 51:50–56

El-Gohary ZMA, Khalifa SA, El-Said Fahmy AM, Tag YM (2011) Comparative studies on the renal structural aspects of the mammalian species inhabiting different habitats. J Am Sci 7:556–565

Gundersen HJ, Bendtsen TF, Korbo L, Marcussen N, Møller A, Nielsen K (1988a) Some new, simple and efficient stereological methods and their use in pathological research and diagnosis. APMIS 96:379–394

Gundersen HJ, Bagger P, Bendtsen TF, Evans SM, Korbo L, Marcussen N, Møller A, Nielsen K, Nyengaard JR, Pakkenberg B, Sorensen FB, Vseterby A, West MJ (1988b) The new stereological tools: dosector, fractionator, nucleator and point sampled intercepts and their use in pathological research and diagnosis. APMIS 96:857–881

Heilmann M, Neudecker S, Wolf I, Gubhaju L, Sticht C, Schock-Kusch D, Kriz W, Bertram JF, Schad LR, Gretz N (2012) Quantification of glomerular number and size distribution in normal rat kidneys using magnetic resonance imaging. Nephrol Dial Transplant 27:100–107

Howard CV, Reed MG (1998) Unbiased stereology: three-dimensional measurement in microscopy. Bios Scientific, Oxford

Jamison RL (1976) Urinary concentration and dilution. In: Brenner BM, Rector FCJR (eds) The kidney. Saunders, Philadelphia, pp 391–441

Kaissling B, Kriz W (1979) Structural analysis of the rabbit kidney. Advances in anatomy. Embryol Cell Biol 56:1–123

Kaplan S, Odaci E, Canan S, Onger ME, Aslan H, Unal B (2012) The disector counting technique. NeuroQuantology 10:44–53

Khazraiinia P, Rostami A, Haddadzadeh HR, Nassiri SM (2008) Hematological characteristics and hemoglobin typing of the Persian squirrel (*Sciurus anomalus*). J Exot Pet Med 17:44–48

Knepper MA, Danielson RA, Saidel GM, Post RS (1977) Quantitative analysis of renal medullary anatomy in rats and rabbits. Kidney Int 12:313–323

Kokko JP (1974) Membrane characteristics governing salt and water transport in the loop of Henle. Fed Proc 33:25–30

Lodrup AB, Karstoft K, Dissing TH, Nyengaard JR, Pederson M (2008) The association between renal function and structural parameters: a pig study. BMC Nephrol 9:18

Malas A, Sulak O, Ungor B, Cetin E, Albey S (2002) Determination of the volume of renal morphological structure by stereological methods. SDU Tp Fak Derg 9:1–5

Mandarim-de-Lacerda CA (2003) Stereological tools in biomedical research. An Acad Bras Cienc 75:469–486

Nyengaard JR (1999) Stereologic methods and their application in kidney research. J Am Soc Nephrol 10(5):1100–1123

Nyengaard JR, Bendtsen TF (1990) A practical method to count the number of glomeruli in the kidney as exemplified in various animal species. Acta Stereol 9:243–258

Rasch R, Dorup J (1997) Quantitative morphology of the rat kidney during diabetes mellitus and insulin treatment. Diabetologia 40:802–809

Silva MA, Merzel J (2001) Stereological determination of the volume of the rat hemimandible tissues. Anat Rec 263:255–259

Soleimani M, Tavakolyan Z (2013) Stereological study of the effect of vitamin E on rat kidney tissue treated with para-nonylphenol. J Cell Tissue 3:297–306

Sterio DC (1984) The unbiased estimation of number and size of arbitrary particles using the disector. J Microsc 134:127–136

Tavafi M, Ahmadvand H, Tamjidipoor A, Delfan B, Khalatbari AR (2011) Satureja khozestanica essential oil ameliorates progression of diabetic nephropathy in uninephrectomized diabetic rats. Tissue Cell 43:45–51

Tsushima Y, Blomley MJ, Okabe K, Tsuchiya K, Aoki J, Endo K (2001) Determination of glomerular filtration rate per unit renal volume using computerized tomography: correlation with conventional measures of total and divided renal function. J Urol 165:382–385

Veshkini A, Tavana M, Sohrab Haghdost I, Nasroulah zadeh Masouleh M, Hbib Savojbolaghi S (2011) Excretory urography by subcutaneous injection of Iodixanol in Persian squirrel (*Sciurus Anomalous*). Pak Vet J 31:17–22

Weissenberg S, Shkolnik A (1994) Metabolic rate and water economy in the desert and Mediterranean populations of the common spiny mouse (*Acomys cahirinus*) in Israel. Isr J Zool 40:135–143